Corona-Discharge-Initiated Mine Explosions

H. K. Sacks, *Senior Member, IEEE,* and Thomas Novak, *Fellow, IEEE*

***Abstract*—Strong circumstantial evidence suggests that lightning has initiated methane explosions in abandoned and sealed areas of underground coal mines. The Mine Safety and Health Administration (MSHA) investigated several of these occurrences within recent years. The investigated explosions occurred at significant depths, ranging from 700 to 1200 ft. Data from the National Lightning Detection Network indicated a strong correlation between the times and locations of the explosions with those of specific lightning strikes. This paper proposes that corona discharge from a steel borehole casing is the most likely mechanism responsible for these ignitions. A recently investigated mine explosion and fire at a depth greater than 1000 ft was selected for this study. Computer simulations were performed, using data collected at the mine site. CDEGS software from Safe Engineering Services & Technologies, Ltd. and MaxwellSV from Ansoft Corporation were used for the simulations.**

***Index Terms*—Coal mining, lightning, methane explosions.**

I. Introduction

ELECTRICAL shock, visible sparking from underground equipment, premature detonation of explosives, and methane explosions have been experienced in underground mines during thunderstorms. These incidents have been particularly well documented in shallow coal mines in South Africa [1]–[3], with the vast majority occurring at mining depths of 300 ft or less. In recent years, several methane explosions in the United States have also been attributed to lightning. However, these explosions occurred at depths ranging from 700 to 1200 ft, which are significantly deeper than any of the incidents experienced in South Africa.

The explosions in the United States took place in abandoned areas of underground coal mines. In all instances, steel-cased boreholes were located in the vicinity of the explosions. Data obtained from The National Lightning Detection Network were useful in determining the number and magnitude of cloud-to-earth lightning strikes within a 10-mi radius of the explosion areas at the estimated times of the explosions [4].

An explosion can occur if lightning dissipates sufficient energy in a methane/air mixture with the methane content between 5%–15%, provided the oxygen content is at least 12%. The minimum energy requirement of only 0.3 mJ occurs with a methane concentration of 8.5%, and pockets of explosive methane/air mixtures can occur in abandoned, and even sealed, areas of coal mines.

Lightning can penetrate an underground mine by two mechanisms—propagation through the overlying strata and conduction through metallic structures extending from the surface to the mine. With the first mechanism, a lightning strike at the surface propagates downward through the earth in a radial fashion. Analyses of tunneling accidents in the Swiss Alps show that lightning strikes are capable of penetrating significant depths of overburden with enough energy to detonate explosives [5]. The depth of penetration was shown to be proportional to soil resistivity. Uniformly elevating the soil's potential, with respect to remote earth, by itself may not necessarily create problems since potential differences are not present in localized areas. However, large conductive structures that are grounded at remote locations can distort local current distributions and result in potential gradients. Geological faults may also significantly distort current distribution through the overburden.

The second lightning-penetration mechanism results from a direct strike or a nearby strike that couples to a metallic structure that extends from the surface to the mine, such as cables, conveyor structures, water pipes, and borehole casings. This mechanism is far more likely in the deep mine incidents in the U.S. The attenuation of such a strike depends on the surge impedance of the structure and how effectively the structure is grounded. In previous research [6], rails from an underground transportation system were modeled as conductors grounded at remote locations to act as the second electrode of a spark gap. In contrast, this paper addresses the possibility of a totally different mechanism, *corona discharge*, as an ignition source. If corona ignition is possible, an actual spark gap is not necessary to create an explosion. The analysis in this paper is based on an actual gob explosion. A brief description of this incident follows.

II. Recent Mine Explosion

On August 31, 2003, a series of thunderstorms produced a total of 83 lightning strikes-to-ground within a 5-mi radius of a longwall-mining panel at a coal mine in West Virginia. Several of these strikes occurred on or near surface gas-transmission lines that connect degasification wells on the mine property. At approximately 4:59 p.m., a pressure spike was recorded at the bleeder ventilation fan, indicating a possible explosion [7]. Shortly afterwards, additional pressure spikes were recorded at both the bleeder and main ventilation fans.

Paper PID-05-02, presented at the 2004 Industry Applications Society Annual Meeting, Seattle, WA, October 3–7, and approved for publication in the IEEE TRANSACTIONS ON INDUSTRY APPLICATIONS by the Mining Industry Committee of the IEEE Industry Applications Society. Manuscript submitted for review October 15, 2004 and released for publication June 9, 2005. This work was supported by the National Institute of Occupational Safety and Health (NIOSH), Pittsburgh Research Laboratory, under Contract 200-2002-000589, *Reduction of Mining Electrical Hazards Through Improved Engineering Controls*.

H. K. Sacks is at 221 Trinity Drive, Canonsburg, PA 15317 USA (e-mail: hksacks@verizon.net).

T. Novak is with the Department of Mining and Minerals Engineering, Virginia Polytechnic Institute and State University, Blacksburg, VA 24061 USA (e-mail: tomnovak@vt.edu).

Digital Object Identifier 10.1109/TIA.2005.853387

TABLE I
LIGHTNING DATA PRIOR TO THE FIRST PRESSURE PULSE

No.	Time	Magnitude [kA]	No	Time	Magnitude [kA]
1	16:22:13	-10.00	25	16:56:10	-31.60
2	16:27:00	-26.50	26	16:56:10	-14.80
3	16:30:41	-10.30	27	16:56:31	-36.50
4	16:35:47	-13.70	28	16:56:42	-23.50
5	16:35:48	-8.60	29	16:56:42	-18.80
6	16:35:48	-12.00	30	16:57:00	-24.80
8	16:49:38	-16.10	31	16:57:00	-13.40
9	16:51:50	-12.70	32	16:57:00	-11.70
10	16:52:06	-12.70	33	16:57:18	-28.00
11	16:52:26	-13.00	34	16:57:18	-14.50
12	16:52:36	-12.90	35	16:57:42	-37.50
13	16:52:57	-10.40	36	16:57:42	-7.30
14	16:53:17	-16.90	37	16:58:03	-26.00
15	16:53:33	-17.90	38	16:58:19	-14.90
16	16:53:33	-11.00	39	16:58:19	-14.70
17	16:53:47	-22.00	40	16:58:19	-7.20
18	16:54:05	-23.00	41	16:58:19	-5.70
19	16:54:05	-12.10	42	16:58:47	-36.60
20	16:54:31	-16.90	43	16:58:47	-9.40
21	16:54:57	-35.10	44	16:59:20	-45.70
22	16:55:19	21.70	45	16:59:20	-38.60
23	16:55:48	-15.20	Pressure Pulse Occurred on Fan Chart at 16:59:40		
24	16:55:48	-18.10			

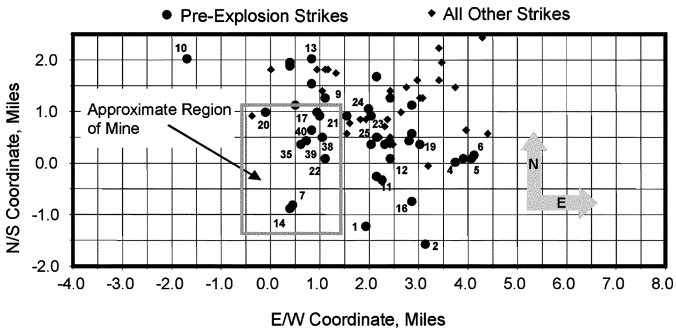

Fig. 1. Geographical location of lightning strikes.

A lightning report [8] for the 24-h period, beginning at 12:00 a.m. on August 31, 2003, was commissioned by the operator of the mine on the suspicion that lightning was responsible for the explosion(s). Table I shows reported data on the lightning strikes prior to the first recorded pressure spike of the fan, and Fig. 1 depicts the geographical locations of these strikes. Fig. 2 illustrates the data superimposed on the mine map. The map also shows the location of degasification wells and the network of gas pipelines interconnecting the wells on the surface. Lightning strikes in Fig. 2 are indicated by small dots while strikes that occurred before the first pressure pulse are marked with doughnuts. The gray 500-m radius rings surrounding the dots represent the strike location uncertainty. Borehole 8HI-1 was actively extracting gas at the time of the thunderstorm and was close to the area where the explosion was thought to have occurred [7]. From Table I, the largest strike in the vicinity of the mine had a peak current magnitude of 38.6 kA. Because of the unknown propagation delay for the pressure pulse through the gob area of the mine, along with the uncertain accuracy of the clock used for recording pressure data at the fan, it is impossible to precisely correlate a specific lightning strike with the recorded pressure pulse.

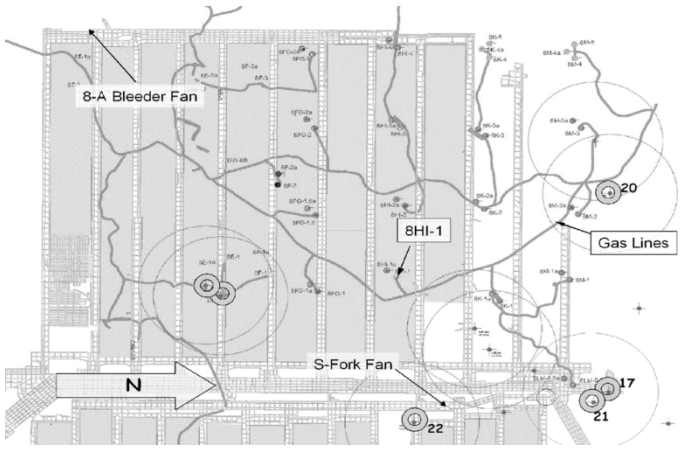

Fig. 2. Mine map showing lightning, boreholes, and gas lines.

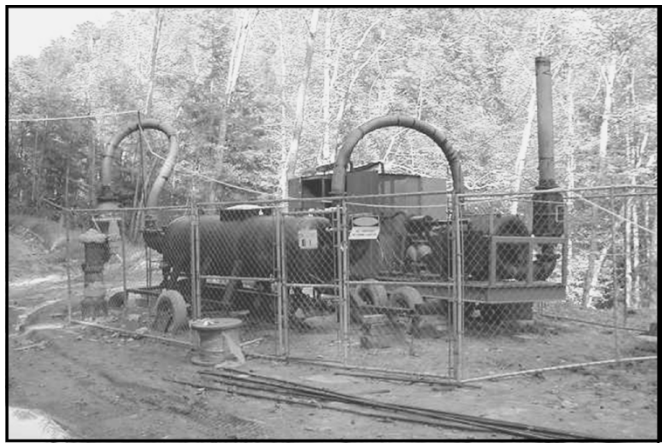

Fig. 3. Degasification well and associated exhaust system.

III. CORONA DISCHARGE

Fig. 3 is a photograph of a gob gas well installation, with the well casing and its attached flame arrester in the left corner, and Fig. 4 depicts a typical gob-gas drainage well. The metal borehole casing extends into the caved zone of the mine. Normally, this zone would have a very high (in the nonflammable range) concentration of methane, but the possibility of a flammable mixture cannot be ruled out since mine air may also be drawn into the zone. If a flammable mixture is present in the vicinity of the pipe, an ignition is possible if sufficient energy is induced into the casing by a lightning strike. In previous work [6], the proposed mechanism was a spark between a roof bolt near the casing, and a grounded haulage rail. While this scenario is possible, there is a much more direct mechanism which does not require the presence of a nearby remotely grounded conductor. Any conductor which is elevated in potential relative to remote ground will be the source of an electric field. If this field exceeds a critical level within the surrounding gas, corona discharge will occur. In air, spark discharge is generally considered to occur at approximately 3000 kV/m. However, corona discharge typically occurs at much lower fields on the order of 500–1000 kV/m [9],

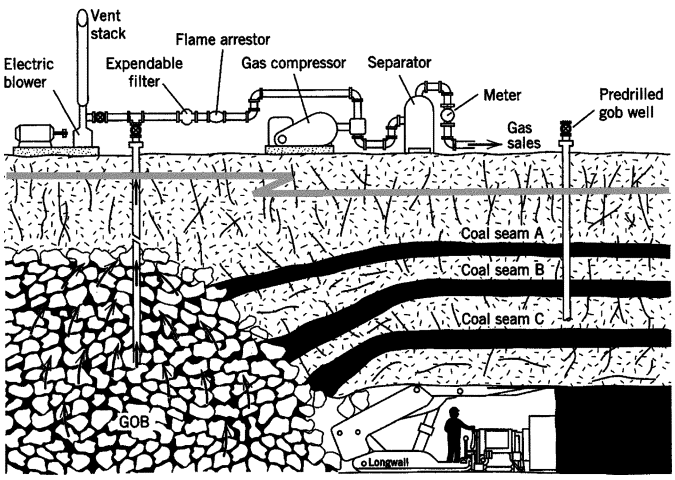

Fig. 4. Rendition of a gob degasification system.

[10]. The discharge consists of a cloud of ionized gas and electrons (plasma).

The actual critical field at which corona forms is a function of the surface geometry, whether the potential is dc or time varying, and properties of the surrounding gas [11].

Experimental research reported in [9] shows that short-duration corona discharges of 50 ns are capable of igniting methane/air mixtures at atmospheric pressure. In fact, such discharges are more efficient than spark discharges (i.e., require less expended energy) and can form the basis of an efficient internal methane/air combustion engine [12]. The remainder of this paper will demonstrate through computer analysis that conditions for corona ignition at the bottom of a borehole casing can be induced from a lightning strike.

IV. Computer Modeling

Two commercially available software packages were used to perform the modeling and analysis—CDEGS and Ansoft MaxwellSV. The CDEGS software uses a double-exponential current surge to simulate a lightning strike that is injected into a borehole casing at the surface. It performs a fast Fourier transform (FFT) to convert the lightning strike from the time domain to its frequency domain. Current distributions, scalar potentials, and electromagnetic fields are computed for selected frequencies at specified observation points. This information provides insight into the frequency response of the earth and associated metal conductors. An inverse FFT is then used to obtain time-domain representations for potentials and fields at any defined point in the system. Computational methods for the CDEGS software can be found in [13]–[15]. The CDEGS software is used to determine the conductor potential and electric field at a specified depth and for a given soil resistivity. The CDEGS software cannot, however, account for the specific, detailed geometry at the end of the borehole casing which can significantly affect the localized electric field strength. By ignoring the time-varying field quantities, Ansoft MaxwellSV software was used to model the electrostatic case in order to investigate the effects caused by the sharp edges of the casing. Although it has no bearing on the analyses, it should also be noted that once ionization begins near the casing, neither model accounts for the space-charge effects.

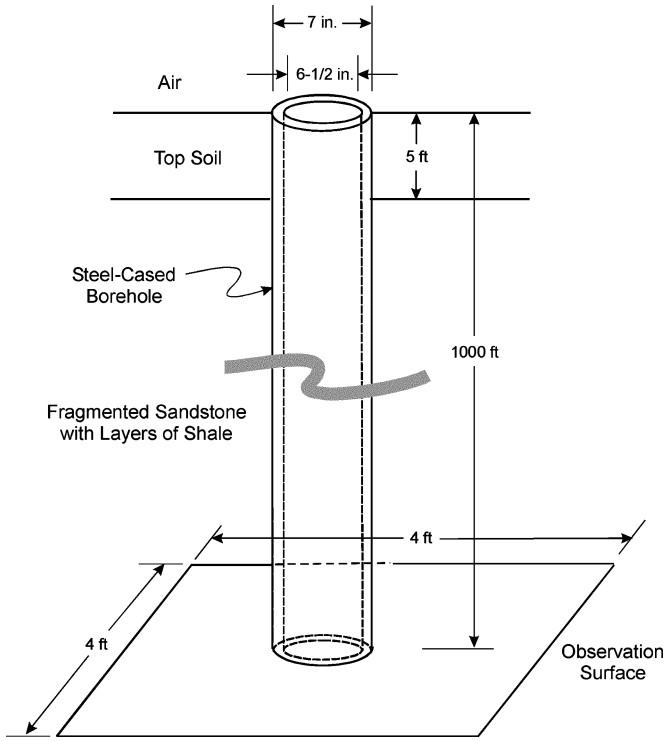

Fig. 5. Physical model for CDEGS analysis.

A. Physical Model

Typical overburden consists of many layers of various types of strata, and the resistivity of each layer can vary dramatically. The composition of overburden is site specific, and discontinuities and geological faults can affect its electrical properties. However, to make the problem manageable, a two-layer model, with constant resistivities, is used to model the overburden. A simple model of a steel-cased borehole embedded in overburden is shown in Fig. 5. The vertical length of the borehole casing is assigned a value of 1000 ft, which is a typical length used at the subject mine. The steel casing is modeled as a 7-in-diameter pipe with an interior diameter of 6.5 in. The casing is assigned a relative resistivity of 17 $(2.93 \times 10^{-7}\ \Omega - \mathrm{m})$ and a relative permeability of 300 $(3.77 \times 10^{-4}\ \mathrm{H/m})$. The top layer of the two-layer soil model is assigned a typical resistivity of 400 $\Omega \cdot \mathrm{m}$ with a depth of 5 ft. The overburden beneath the top soil consists primarily of sandstone with some layers of shale. Homogeneous sedimentary rock, such as sandstone, has a wide range of resistivities that depend upon the rock's composition and moisture content. The resistivity for sandstone can vary from $1.0 \times 10^5\ \Omega \cdot \mathrm{m}$ to $1.0 \times 10^7\ \Omega \cdot \mathrm{m}$, with a relative permittivity of 7.0 $(6.20 \times 10^{-11}\ \mathrm{F/m})$ [16]. However, the sandstone in the overburden of the subject mine is significantly fractured with a major portion lying below the local area's water table. To accommodate the variations in overburden resistivity, simulations were performed over a range from $1.0 \times 10^3\ \Omega \cdot \mathrm{m}$ to $1.0 \times 10^5\ \Omega \cdot \mathrm{m}$. Using a range of values also reveals the effect

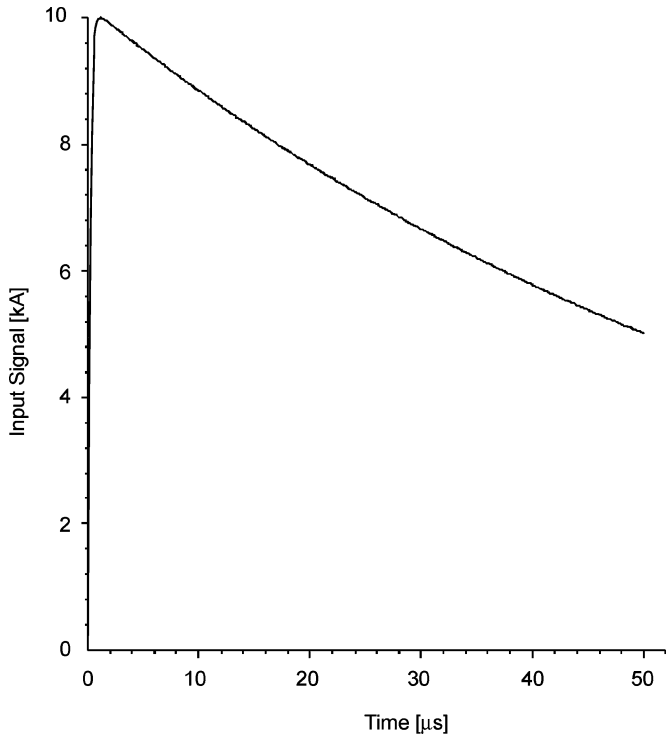

Fig. 6. Model of lightning current for CDEGS analysis.

of overburden resistivity on the lightning-induced potential and electromagnetic fields near the bottom of the borehole casing.

B. Lightning Surge

The lightning surge is modeled as a current source with the following double exponential function:

$$I(t) = I_m[e^{-\alpha t} - e^{-\beta t}].$$

The values of α and β can be adjusted to cause a rise time of 1.2 μs to a peak-current value I_m, and a subsequent decay to 50% of its peak value at 50 μs. This type of waveform is typically used for modeling lightning strikes [17]. A plot of a 10-kA lightning waveform, which is used for easy scaling, is shown in Fig. 6. The following coefficients are used to obtain the desired rise and decay times:

$$\alpha = 1.42 \times 10^4$$
$$\beta = 4.88 \times 10^6.$$

Fig. 7 shows a general frequency spectrum for the waveform of Fig. 6. The rapid rise time of the lightning waveform results in large current components between dc and 100 kHz, with smaller components occurring well into the megahertz range.

C. Time-Varying Simulations

The CDEGS software uses a forward FFT to decompose the time-domain lightning surge of Fig. 6 into its frequency spectrum. It then selects a finite number of frequencies from this spectrum, based on the electromagnetic field response in the frequency domain. Additional frequencies with finer steps are selected in the regions where rapid changes in magnitude occur. Electromagnetic fields are computed for defined observation points at each selected frequency to obtain the frequency spectrum of the fields. Finally, an inverse FFT is applied to the frequency spectrum of the computed electromagnetic fields, at the defined observation points, to yield the time-domain responses of the fields. A sample simulation is performed for the physical model and lightning strike previously described.

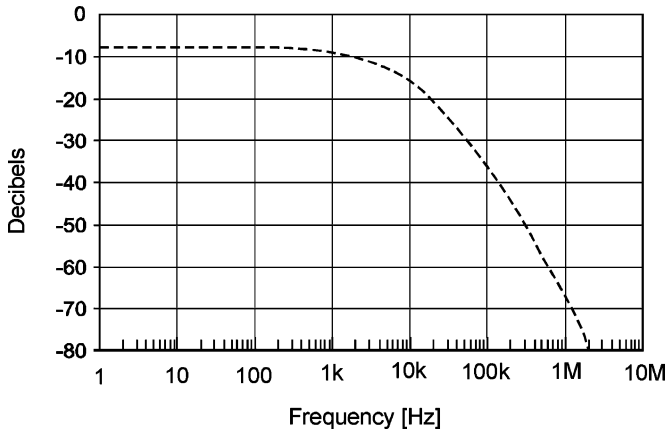

Fig. 7. Frequency spectrum for a 1.2/50-μs waveform.

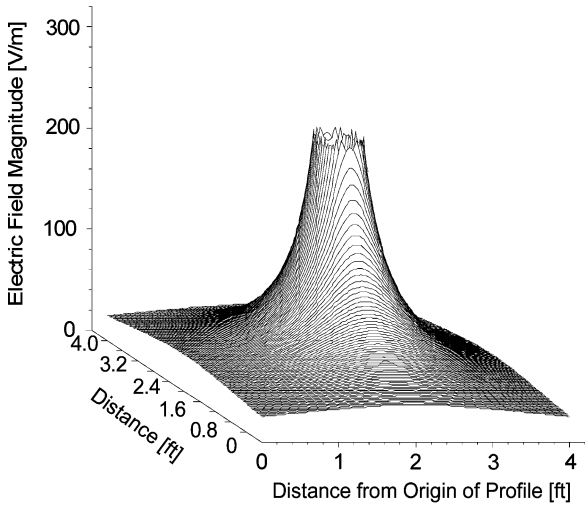

Fig. 8. Electric field for per-unit dc current.

The frequency spectrum of the lightning surge in Fig. 6 varies from dc to the megahertz range. The waveform of Fig. 6 is modeled from 0 to 900 μs, even though it essentially decays to 0 A well before 600 μs. For the FFT, 2^{13} (8192) samples are taken, which results in a Nyquist frequency of 4.55 MHz. This frequency is then defined as the highest frequency for determining the response of the system. The model's unmodulated frequency response can be depicted in three dimensions for any frequency. As an example, Fig. 8 shows the dc response on the observation surface when a per-unit current of $1.0 + j0.0$ A is injected into the top of the borehole, and the overburden resistivity is $1.0 \times 10^5\ \Omega \cdot$ m. The magnitude of the dc electric field is calculated at each of the intersection points on a predefined grid of the observation surface, which is illustrated in Fig. 8.

As anticipated, the electric field goes to zero in the interior of the borehole casing. Its peak value of approximately 260 V/m occurs at the exterior surface and decays in an outward radial

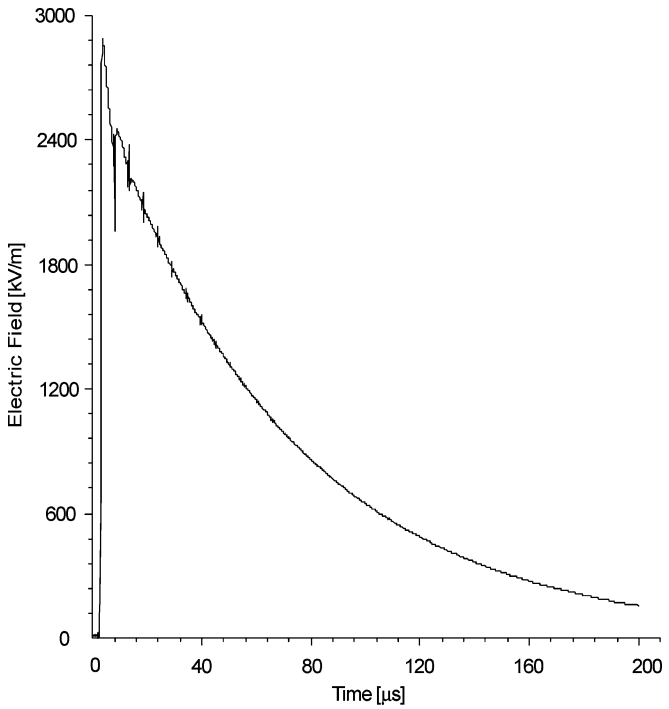

Fig. 9. Time-varying electric field at bottom of casing.

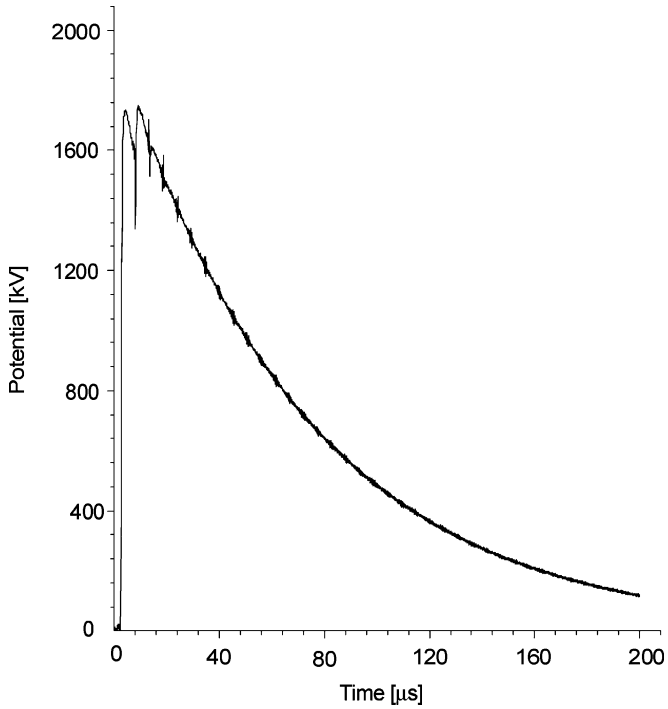

Fig. 10. Time-varying potential at bottom of casing.

direction from the casing. The per-unit responses of many hundreds of frequencies are used to reconstruct the overall time-domain response of the fields and potentials. These per-unit responses are referred to as the unmodulated frequency response. The CDEGS software continuously suggests frequencies, primarily at points where rapid changes in magnitude occur, until the changes are well defined. The well-defined plots allow the software to perform interpolations to obtain the required remaining frequencies for calculating the inverse FFT.

The resulting time-varying plots for the electric field and scalar potential at a point on the surface of the casing are presented in Figs. 9 and 10, respectively. Again, these results are based on a 10-kA lightning strike and a $1.0 \times 10^5\ \Omega \cdot \mathrm{m}$ overburden resistivity. Fig. 11 shows the peak voltage at the bottom of the borehole casing for strike currents from 10 to 50 kA for various overburden resistivities.

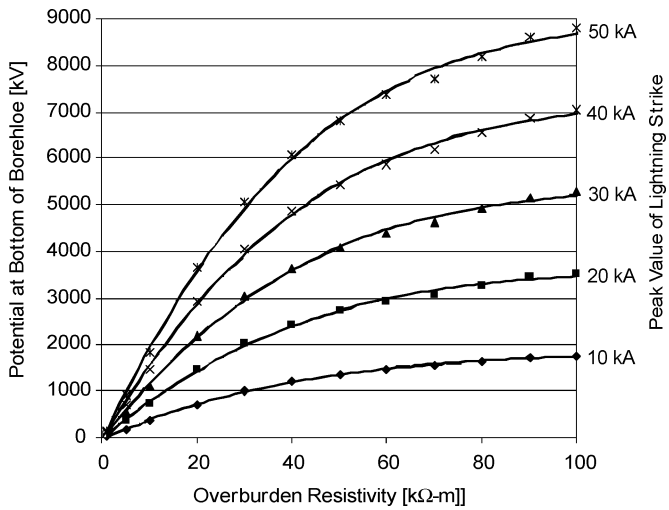

Fig. 11. Peak voltages at bottom of borehole as a function of overburden resistivity and lightning-strike current.

D. Electrostatic Simulations

Ansoft MaxwellSV Software was used to develop and analyze a borehole model from an electrostatic perspective. As in the previous example, the surrounding rock is assumed to have a relative permittivity of 7.0 and a resistivity of $1.0 \times 10^5\ \Omega \cdot \mathrm{m}$. The electrostatic model is shown in Fig. 12. The casing extends 12 in below the rock into the mine void. A ground plane was initially placed 10 ft below the bottom of the rock layer. A second series of calculations was run with the ground plane receding to infinity.

The casing is assigned a uniform potential of 1 Vdc with respect to ground. Figs. 13 and 14 show the magnitudes of the electric fields surrounding the end of the borehole casing with the ground plane located 10 ft below the casing and then receding to infinity, respectively. The casing's right wall is shown in cross section in black. The figures clearly show the highest electric field strength occurring at the edges of the casing. When the ground plane recedes to infinity, the general characteristics of the electric field are unchanged. This is also the case most likely to exist in the mine. While higher field strengths obviously exist closer to the edges, some minimum volume of gas must exist within the influence of the electric field for an ignition to propagate. For example, 30 CFR § 7.304[1] requires that the air gap between the end of a cylindrical surface and a plane be no more than 0.008 in. This is based on experimental evidence that a methane/air flame will not propagate through such a gap and is the result of cooling of the escaping combustion products by the metal surfaces. In the borehole situation, there is no mating surface, which strongly suggests that a layer of burning gas, as

[1]Code of Federal Regulations for Explosion Proof Enclosures used in methane–air atmospheres. Such enclosures will not allow a flame to propagate from within the enclosure to the surrounding explosive atmosphere.

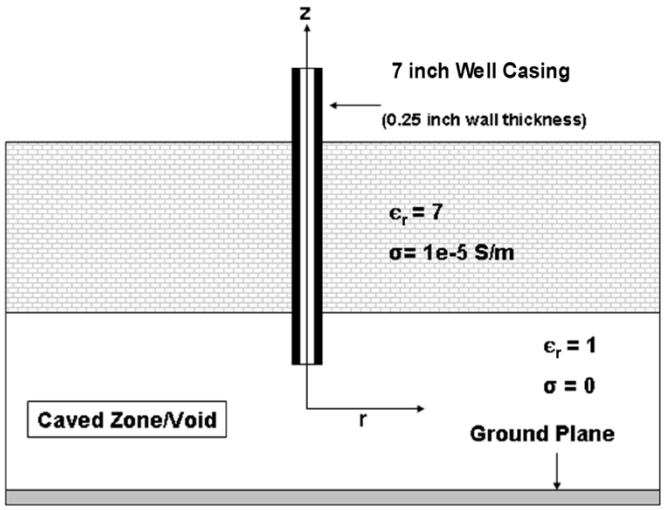

Fig. 12. Electrostatic model of borehole casing.

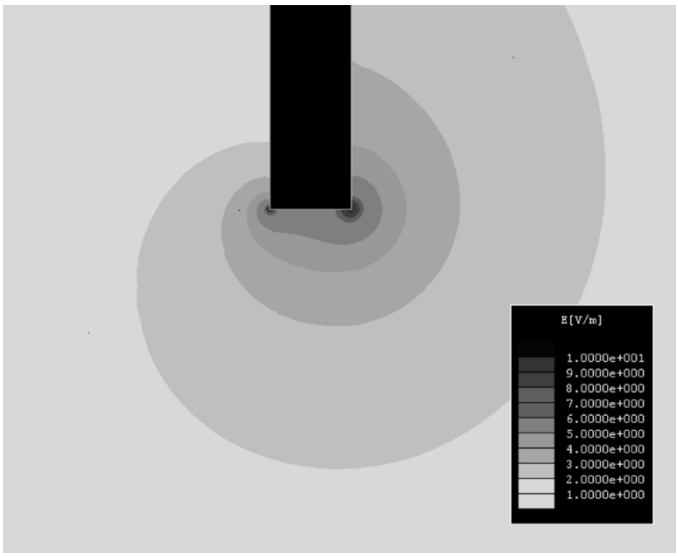

Fig. 13. Electric field plot with 1 Vdc applied to the casing and the ground plane at 10 ft below casing.

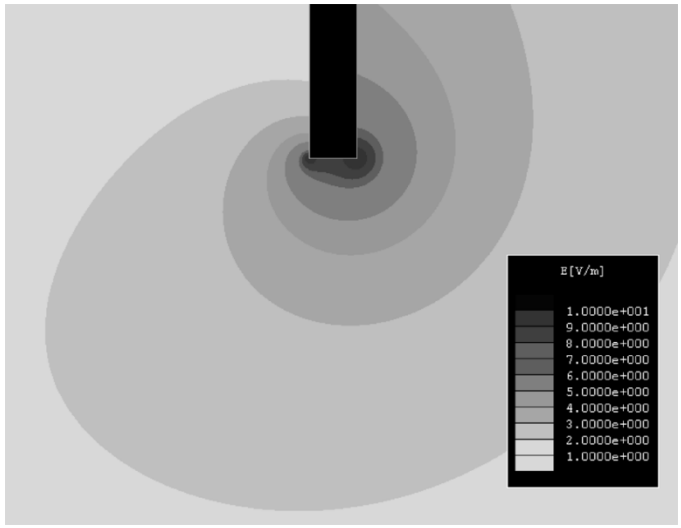

Fig. 14. Electric field plot with 1 Vdc applied to the casing and the ground plane receded to infinity.

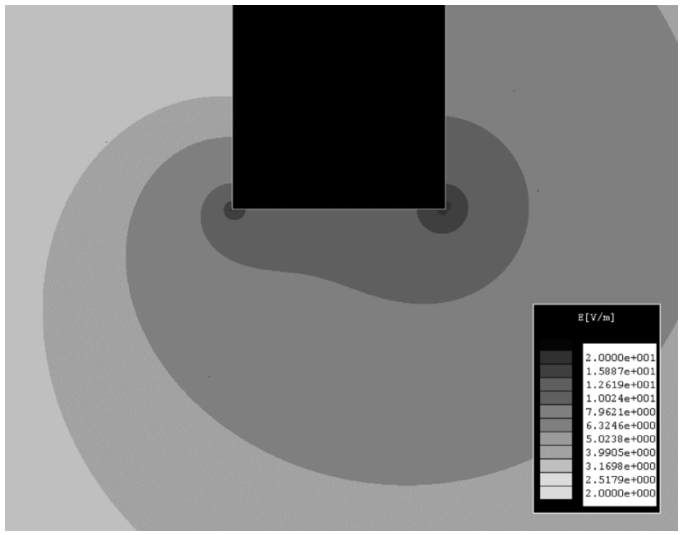

Fig. 15. Magnified view of Fig. 14.

thin as 0.008 in, will continue to propagate. Fig. 15 is a magnified view of the field and shows that at distances of ∼10% of the wall thickness (∼0.025 in) the field exceeds 10 V/m for 1 Vdc on the casing. Since corona discharge can occur at field strengths of 1000 kV/m, the minimum voltage for corona formation is approximately 100 kV on the casing. Fig. 11 illustrates that, except for the weakest strikes and lowest overburden resistivities, corona discharge is likely to occur.

V. Conclusion

Strong circumstantial evidence suggests that lightning has initiated methane explosions in abandoned and sealed areas of deep underground coal mines. Steel-cased boreholes that extended from the surface to the mine level were present in all cases. Past research was directed toward electrical arcing as the ignition source, which requires two separate electrodes—the borehole casing and some remotely grounded conductor. The authors propose a more feasible and direct mechanism—*corona discharge*. Computer simulations were performed to support this hypothesis. CDEGS software from Safe Engineering Services & Technologies, Ltd. (SES) was first used to obtain potentials at the bottom of a 1000-ft steel-cased borehole as a function of overburden resistivity and the magnitude of the lightning strike. The casing was assumed to have a 7-in outer diameter and a 1/4-in wall thickness. The overburden was modeled in two layers. A 5-ft layer of topsoil with a resistivity of 400 $\Omega \cdot$ m was used for the first layer, and the remaining overburden was modeled as sedimentary rock using resistivities ranging from 1.0×10^3 to 1.0×10^5 $\Omega \cdot$ m. The lightning strike was modeled as a current source with a standard 1.2/50-μs waveform. The results of the CDEGS simulations show that overburden resistivity significantly influences the magnitude of the voltage at the bottom of the borehole casing—the potential increases as the overburden resistivity increases. Although the CDEGS software can determine the time-varying electric field at the surface of the casing, it does not account for the detailed geometry at the end of the casing which can significantly affect the

electric field strength. Therefore, MaxwellSV from Ansoft Corporation was used to investigate these effects from an electrostatic perspective at the bottom of the casing which extends into the mine void. These simulations clearly show that the highest electric field strength occurs at the sharp edges of the casing. The simulations further show that, within distances of $\sim$10% of the casing's wall thickness, an electric field over 10 V/m occurs when a uniform 1.0-Vdc potential is applied to the casing. Since corona is initiated when an electric field exceeds approximately 1000 kV/m, the minimum casing potential for corona formation is approximately 100 kV. The results obtained from the CDEGS simulations further show that corona discharge is likely to occur except for extremely weak lightning strikes and extremely low overburden resistivities.

REFERENCES

[1] H. J. Geldenhuys, A. J. Eriksson, W. B. Jackson, and J. B. Raath, "Research into lightning-related incidents in shallow South African coal mines," in *Proc. 21st Int. Conf. Safety in Mines Research Institutes*, Sydney, Australia, Oct. 1985, pp. 775–782.

[2] H. J. Geldenhuys, "The measurement of underground lightning-induced surges in a colliery," in *Proc. Symp. Safety in Coal Mining*, Pretoria, South Africa, Oct. 1987, pp. 1–13.

[3] K. A. Zeh, "Lightning and safety in shallow coal mines," in *Proc. 23rd Int. Conf. Safety in Mines Research Institutes*, Washington, DC, Sept. 1989, pp. 691–700.

[4] E. L. Checca and D. R. Zuchelli, "Lightning strikes and mine explosions," in *Proc. 7th U.S. Mine Ventilation Symposium*, 1995, pp. 245–250.

[5] K. Berger, *Protection of Underground Blasting Operations*, R. H. Golde, Ed. London, U.K.: Academic, 1977, vol. 2, Lightning, ch. 20.

[6] T. Novak and T. Fisher, "Lightning propagation through the Earth and its potential for methane ignitions in abandoned areas of coal mines," *IEEE Trans. Ind. Appl.*, vol. 37, no. 6, pp. 1555–1562, Nov./Dec. 2001.

[7] "Pinnacle Mine—Non-injury explosion," Mine Safety and Health Administration, Triadelphia, WV, Internal Rep., 2003.

[8] "Strikenet Rep. LA46060," Vaisala, Inc., Woburn, MA, Aug. 31, 2003.

[9] J. B. Liu, P. D. Ronney, and M. A. Gundersen, "Premixed flame ignition by transient plasma discharges," presented at the 29th Int. Symp. Combustion, Sapporo, Japan, Jul. 21–26, 2002.

[10] E. M. Bazelyan and Y. P. Raizer, Eds., *Spark Discharge*. New York: CRC Press, 1998, p. 5.

[11] D. G. Fink and H. W. Beaty, *Standard Handbook for Electrical Engineers*, 12th ed. New York: McGraw-Hill, 1987, pp. 4–136.

[12] P. Ronney, N. Theiss, J. B. Liu, and M. Gundersen, "Corona discharge ignition for advanced stationary natural gas engines," presented at the ASME-ICED'04, Long Beach, CA, Oct. 24–27, 2004, Paper 891.

[13] A. Selby and F. P. Dawalibi, "Determination of the current distribution in energized conductors for the computation of electromagnetic fields," *IEEE Trans. Power Del.*, vol. 9, no. 2, pp. 1069–1078, Apr. 1994.

[14] F. P. Dawalibi and A. Selby, "Electromagnetic fields of energized conductors," *IEEE Trans. Power Del.*, vol. 8, no. 3, pp. 1275–1284, Jul. 1993.

[15] F. P. Dawalibi, W. Ruan, and S. Fortin, "Lightning transient response of communications towers and associated grounding networks," in *Proc. ICEMC'95 KUL*, Kuala Lumpur, Malaysia, Apr. 11–13, 1995, pp. 95–102.

[16] E. I. ParkhomenkoI, *Electrical Properties of Rocks*. New York: Plenum, 1967, p. 38, 111.

[17] D. W. Zipse, "Lightning protection systems: advantages and disadvantages," *IEEE Trans. Ind. Appl.*, vol. 30, no. 5, pp. 1351–1361, Sep./Oct. 1994.

H. K. Sacks (S'62–M'68–SM'03) received the B.S.E.E. degree from the University of Maryland, College Park, and the M.S. and Ph.D. degrees in electrical engineering from Carnegie Mellon University, Pittsburgh, PA. He also received the M.B.A. degree from the University of Pittsburgh, Pittsburgh, PA, in 1982.

He is an Adjunct Research Professor at Virginia Polytechnic Institute and State University, Blacksburg. Formerly, he was the Deputy Research Director at the Pittsburgh Research Laboratory of the U.S. Bureau of Mines [now part of the National Institute for Occupational Safety and Health (NIOSH)]. While at NIOSH, he researched the economic costs of occupational injuries and methods to prevent electrical injuries in mining. In 2003, he was awarded a patent on a method to prevent electrical injuries associated with the contact of mobile equipment with high-voltage transmission lines.

Dr. Sacks is a Member of the Mining Industry Committee of the IEEE Industry Applications Society.

Thomas Novak (M'83-SM'93–F'05) received the B.S. degree in electrical engineering from The Pennsylvania State University, University Park, in 1975, the M.S. degree in mining engineering from the University of Pittsburgh, Pittsburgh, PA, in 1978, and the Ph.D. degree in mining engineering from The Pennsylvania State University in 1984.

He is presently the C.T. Holland Professor and Department Head of Mining and Minerals Engineering at Virginia Polytechnic Institute and State University (Virginia Tech), Blacksburg. Prior to joining Virginia Tech, he was the Department Head and holder of the Drummond Endowed Chair of Civil Engineering at The University of Alabama, Tuscaloosa., where he also held the positions of Interim Department Head of Aerospace Engineering and Mechanics, Professor of Electrical Engineering, and Associate Professor of Mineral Engineering. He has also worked as an Instructor of Mining Engineering at The Pennsylvania State University; an Electrical Engineer for the U.S. Bureau of Mines, Pittsburgh Research Center; and Assistant Division Maintenance Engineer for the Republic Steel Corporation, Northern Coal Mines Division.

Dr. Novak has served as a Member of the Executive Board of the IEEE Industry Applications Society (IAS) and was Chairman of its Meetings Department (2000–2002) and Chairman of its Process Industries Department (1994–1998). He also served as Chairman (1992–1994) and Vice-Chairman (1990–1992) of the Mining Industry Committee of the IAS, and Co-chairman of the Mining Industry Technical Conference (1987). He is a Member of the Society of Mining, Metallurgy, and Exploration, Inc. (SME) and is a Licensed Professional Engineer in the States of Alabama and Pennsylvania.